Combined Effects of Ocean Acidification and Light or Nitrogen Availabilities on ^{13}C Fractionation in Marine Dinoflagellates

Mirja Hoins[1,2]*, Tim Eberlein[2], Christian H. Großmann[2], Karen Brandenburg[2], Gert-Jan Reichart[1,4], Björn Rost[2], Appy Sluijs[1], Dedmer B. Van de Waal[3]

1 Department of Earth Sciences, Utrecht University, Utrecht, The Netherlands, 2 Marine Biogeosciences, Alfred Wegener Institute Helmholtz Centre for Polar and Marine Research, Bremerhaven, Germany, 3 Department of Aquatic Ecology, Netherlands Institute of Ecology (NIOO-KNAW), Wageningen, The Netherlands, 4 Geology Department, Royal Netherlands Institute for Sea Research (NIOZ), Den Hoorn (Texel), The Netherlands

* mhoins@awi.de

Abstract

Along with increasing oceanic CO_2 concentrations, enhanced stratification constrains phytoplankton to shallower upper mixed layers with altered light regimes and nutrient concentrations. Here, we investigate the effects of elevated pCO_2 in combination with light or nitrogen-limitation on ^{13}C fractionation (ε_p) in four dinoflagellate species. We cultured *Gonyaulax spinifera* and *Protoceratium reticulatum* in dilute batches under low-light ('LL') and high-light ('HL') conditions, and grew *Alexandrium fundyense* and *Scrippsiella trochoidea* in nitrogen-limited continuous cultures ('LN') and nitrogen-replete batches ('HN'). The observed CO_2-dependency of ε_p remained unaffected by the availability of light for both *G. spinifera* and *P. reticulatum*, though at HL ε_p was consistently lower by about 2.7‰ over the tested CO_2 range for *P. reticulatum*. This may reflect increased uptake of (^{13}C-enriched) bicarbonate fueled by increased ATP production under HL conditions. The observed CO_2-dependency of ε_p disappeared under LN conditions in both *A. fundyense* and *S. trochoidea*. The generally higher ε_p under LN may be associated with lower organic carbon production rates and/or higher ATP:NADPH ratios. CO_2-dependent ε_p under non-limiting conditions has been observed in several dinoflagellate species, showing potential for a new CO_2-proxy. Our results however demonstrate that light- and nitrogen-limitation also affect ε_p, thereby illustrating the need to carefully consider prevailing environmental conditions.

Introduction

Anthropogenic activities have caused the partial pressure of CO_2 (pCO_2) in the atmosphere and oceans to increase at an unprecedented rate [1]. This will shift marine carbon speciation towards increasing CO_2 and bicarbonate (HCO_3^-) concentrations, and decreasing carbonate ion (CO_3^{2-}) concentration and pH [2]. Along with these changes in carbonate chemistry, global

temperatures are expected to rise by 2 to 6°C within this century [1], which likely leads to enhanced (thermal) stratification for most oceanic regions [3]. Enhanced stratification can cause primary production to decrease, as observed in low-latitude oceans [4], where the mixed layer depth is already relatively shallow and upwelling of nutrient-rich deeper water masses is suppressed. Alternatively, enhanced stratification may increase primary production in regions with deep mixed layer depths, such as in high latitude oceans. At such locations, phytoplankton may be light-limited due to the deep convective turnover [5]. Irrespective of the net effect on primary production, shoaling of the thermocline causes phytoplankton to be more often restricted to the upper layers of the water column, characterized by high irradiance and low nutrient concentrations [6]. Such changes in light intensity and nutrient concentration may affect marine phytoplankton, including dinoflagellates.

Dinoflagellates are unicellular eukaryotes and can reach high densities under favorable environmental conditions, which may lead to harmful algal blooms with adverse effects not only for the aquatic food web, but also for human health (e.g. [7; 8]). Strategies that add to their success include toxin production, allelopathy, mixotrophy and cyst formation [9; 10; 11; 12]. While studies have investigated how dinoflagellates are influenced by changes in pH and/or $p\mathrm{CO}_2$ [13; 14; 15; 16; 17], less is known about the combined effects of CO_2 and light availabilities (as daylength, see [18]) or CO_2 and nitrogen-limitation [19]. Like all phytoplankton, dinoflagellates fix CO_2 with the carboxylation enzyme Ribulose-1,5-bisphosphate Carboxylase/Oxygenase (RubisCO), which discriminates between carbon isotopes, favoring $^{12}\mathrm{C}$ over $^{13}\mathrm{C}$ (e.g. [20; 21; 22]). The inorganic carbon (C_i) species taken up by phytoplankton differ in their isotopic composition, with CO_2 being $^{13}\mathrm{C}$-depleted compared to HCO_3^-. Under elevated CO_2 concentrations, dinoflagellates may take up relatively more CO_2, resulting in higher $^{13}\mathrm{C}$ fractionation (ε_p) [23; 14]. Similarly, high CO_2 efflux:total C_i uptake (i.e. leakage) prevents the accumulation of $^{13}\mathrm{C}$ within the intracellular carbon pool, thereby increasing ε_p [23; 14]. Indeed, ε_p values in different phytoplankton groups, including dinoflagellates, were shown to increase with elevated $p\mathrm{CO}_2$ [18; 24; 14; 25; 17].

Organic dinoflagellate cysts are ubiquitously preserved in marine sediments (e.g. [26]). The CO_2 dependency of their isotopic composition may be reflected in their cysts, thus potentially providing a proxy for past CO_2 concentrations. However, the CO_2 dependency in ε_p may be affected by other environmental conditions, such as the availability of light and nutrients (e.g. [27; 28; 29; 30]). Here, we investigate the combined effects of elevated $p\mathrm{CO}_2$ and low-light conditions or nitrogen-limitation on particulate organic carbon (POC) production (μ_c), Chlorophyll-a (Chl-a):POC ratios and ε_p in four marine dinoflagellate species. We grew *Gonyaulax spinifera* and *Protoceratium reticulatum* under low-light conditions (LL) and *Alexandrium fundyense* and *Scrippsiella trochoidea* under nitrogen-limiting conditions (LN) and compared these responses to results from an earlier study, where the same species were grown under high-light and nitrogen-replete conditions (HL and HN).

Materials and Methods

Experimental Set-up

For the high-light and nutrient-replete conditions, experiments were performed as dilute batches with *Gonyaulax spinifera* (strain CCMP 409), *Protoceratium reticulatum* (strain CCMP 1889), *Alexandrium fundyense* (strain Alex5, [31]; previously *A. tamarense* [32]), and *Scrippsiella trochoidea* (strain GeoB267; culture collection of the University of Bremen). Each strain was grown in 2.4 L air-tight borosilicate bottles at a constant temperature of 15°C and dissolved CO_2 concentrations ranging from ~5–50 µmol L^{-1}. CO_2 levels of 180, 380, 800 and 1200 µatm were obtained by mixing CO_2-free air (<0.1 µatm $p\mathrm{CO}_2$, Domnick

Hunter, Willrich, Germany) with pure CO_2 (Air Liquide Deutschland, Düsseldorf, Germany) using mass flow controllers (CGM 2000, MCZ Umwelttechnik, Bad Nauheim, Germany). Each of the pCO$_2$ treatments was performed in biological triplicates (n = 3). Experiments were carried out at low cell densities with final concentrations <400 cells mL^{-1}, ensuring negligible changes in carbonate chemistry of <3.5% with respect to dissolved inorganic carbon (DIC).

As growth medium, filtered North Sea seawater (cellulose acetate membrane, 0.2 μm pore size, Sartorius, Göttingen, Germany) with a salinity of 34 and enriched with 100 μmol L^{-1} nitrate and 6.25 μmol L^{-1} phosphate was used. $FeCl_3$ (1.9 μmol L^{-1}), H_2SeO_3 (10 nmol L^{-1}) and $NiCl_2$ (6.3 nmol L^{-1}) were added according to K medium [33], and metals and vitamins were added according to f/2 medium [34]. Bottles were placed on a roller table in order to avoid sedimentation. Daylight tubes (Lumilux HO 54W/965, Osram, München, Germany) provided incident light intensities of 250 ± 25 μmol photons m^{-2} s^{-1} at a 16:8 h light:dark cycle. In order to determine the carbonate chemistry, pH was measured every other day using a WTW 3110 pH meter equipped with a SenTix 41 Plus pH electrode (Wissenschaftlich-Technische Werkstätten GmbH, Weilheim, Germany), which was calibrated prior to each measurement to the National Bureau of Standards (NBS) scale. The precision of pH measurements during the experiments was ±0.02 units. Cells were acclimated to the pCO$_2$ treatments for at least 7 generations (i.e. >21 days) prior to each experiment.

For the low-light treatments, the same conditions as the nutrient-replete dilute batch conditions were applied, except that incident light intensities were reduced to 55 ± 5 μmol photons m^{-2} s^{-1}. In these incubations, CO_2 concentrations ranged between ca. 16 and 50 μmol L^{-1}, according to pCO$_2$ values of 380, 800 and 1200 μatm. Nitrogen-limited conditions were achieved in gently mixed continuous cultures [35]. Cultures were grown as chemostats with fixed dilution rates representing ~33% of maximum growth for each species, with 0.15 ± 0.01 d^{-1} for *A. fundyense* and 0.2 ± 0.01 d^{-1} for *S. trochoidea*, yielding nitrate concentrations below 0.8 μmol L^{-1} for both species. In these incubations, CO_2 concentrations ranged between ca. 8 and 40 μmol L^{-1}, according to pCO$_2$ values of 220, 800 and 1000 μatm (*A. fundyense*), and 280, 590 and 770 μatm (*S. trochoidea*). Steady state was reached after 22–43 days of acclimation, and samples were taken during this phase over 4 consecutive sampling points with time intervals of 2–3 days. For more details on the setup of the continuous culture experiment we refer to Eberlein et al. [19].

Sampling and Analyses

For total alkalinity (TA) analysis, 50 mL culture suspension was filtered over cellulose acetate syringe filters (0.45 μm pore size, Thermo Scientific, Waltham, Massachusetts, USA) and stored in gas tight borosilicate bottles at 3°C. Samples were then analyzed in duplicates using an automated TitroLine burette system (SI Analytics, Mainz, Germany) with a precision of ±13 μmol L^{-1}. Certified Reference Materials (CRMs) supplied by A. Dickson (Scripps Institution of Oceanography, USA) were used to correct for inaccuracies of TA measurements. TA was measured at the beginning and end of each experiment, and during steady-state conditions in the continuous cultures. Minor changes in TA over the course of the experiments combined with the pH measurements every other day allowed for a complete resolution of the carbonate chemistry. The carbonate chemistry was assessed with the program CO2sys [36] using TA and pH (following recommendations of Hoppe et al. [37]) as well as temperature, salinity and phosphate concentration. We used the dissociation constants of carbonic acid and sulfuric acid of Mehrbach et al. [38], refitted by Dickson and Millero [39] and Dickson [40], respectively.

Duplicate samples of 20 mL culture suspension were fixed with neutral Lugol's solution (2% final concentration) and counted every day or every other day with an inverted light microscope (Axiovert 40C, Zeiss, Germany). Growth rates during the exponential phase of growth were assessed separately for each biological treatment by fitting an exponential function through the cell numbers over time according to:

$$N = N_0 e^{\mu t} \tag{1}$$

with N referring to cell number per mL at time t in days, N_0 to the cell number per mL at the start of the experiment, and μ referring to the specific growth rate (d^{-1}).

At the end of the experiment, when cells where still in exponential growth, we took samples to analyze Chl-a, POC and its isotopic composition ($\delta^{13}C_{POC}$). For the analysis of Chl-a, duplicate samples of 200 mL of culture suspension were filtered over cellulose acetate filters (Whatman, Maidstone, UK). Filters were rapidly frozen in liquid nitrogen and stored at -80°C. Chl-a was extracted using 90% acetone with subsequent sonication for 0.5 min. Fluorescence was assessed using a TD-700 Fluorometer (Turner Designs, Sunnyvale, CA), and Chl-a concentrations were calculated according to Knap et al. [41]. To measure POC and PON quota and $\delta^{13}C_{POC}$, 300–400 mL of culture suspension was filtered over pre-combusted GF/F filters (6 h, 500°C). Filters were stored in pre-combusted glass Petri dishes and 200 μL of HCl (0.2 mol L^{-1}) was added to remove any inorganic carbon before they were dried overnight and stored at -25°C. POC quota and $\delta^{13}C_{POC}$ of dilute batch experiments were then measured in duplicate with an Automated Nitrogen Carbon Analyser mass spectrometer (ANCA- SL 20–20, SerCon Ltd., Crewe, UK), with a precision of ± 0.5 μg C and 0.3‰, respectively. POC and PON quota and $\delta^{13}C_{POC}$ of the continuous cultures were measured with a Delta S (Thermo) isotopic ratio mass spectrometer connected to an elemental analyzer CE1108 via an open split interface (Finnigan Conflow II). $\delta^{13}C_{POC}$ is reported relative to the Vienna PeeDee Belemnite standard (VPDB). μ_c was calculated by multiplying μ with POC quota.

For isotopic measurements of the dissolved inorganic carbon ($\delta^{13}C_{DIC}$), 4 mL of culture suspension was sterile filtered over 0.2 μm cellulose acetate filters (Thermo Scientific, Waltham, Massachusetts, USA) and stored at 3°C. 0.7 mL of the filtrate was then transferred to 8 mL vials, which contained three drops of 102% H_3PO_4 solution, and headspaces filled with helium. After equilibration, the isotopic composition in the headspace was measured using a Gas-Bench-II coupled to a Thermo Delta-V advantage isotope ratio mass spectrometer, with a precision of ±0.1‰. ε_p was calculated relative to the isotopic composition of dissolved CO_2 in the water ($\delta^{13}C_{CO2}$) with an equation modified after Freeman and Hayes [42]:

$$\varepsilon_p = \frac{\delta^{13}C_{CO2} - \delta^{13}C_{POC}}{1 + \frac{\delta^{13}C_{POC}}{1000}} \tag{2}$$

In order to calculate the isotopic composition of CO_2 ($\delta^{13}C_{CO2}$) from $\delta^{13}C_{DIC}$, we calculated the isotopic composition of HCO_3^- ($\delta^{13}C_{HCO3-}$) based on $\delta^{13}C_{DIC}$ according to a mass balance relation following Zeebe and Wolf-Gladrow [43] and the temperature-dependent fractionation factors between CO_2 and HCO_3^- and CO_3^{2-} and HCO_3^-, as determined by Mook et al. [44] and Zhang et al. [45], respectively. For further details on the determination of carbon isotope fractionation we refer to Van de Waal et al. [25].

Statistical analysis

Shapiro-Wilk tests confirmed normality of the data. Linear regressions were used to determine the relations between the tested variables and CO_2. Significant differences between CO_2 treatments were confirmed by one-way ANOVA followed by post hoc comparison of the means

using the Tukey HSD (α = 0.05). A covariance analysis (ANCOVA) was used to determine homogeneity of slopes. When slopes were significantly different, i.e. when there were interactive effects of CO_2 with light or nitrogen, the Johnson-Neyman technique (J-N; Johnson and Neyman [46]) was applied to identify the range of CO_2 over which the investigated parameter was different. To improve the homogeneity of variances, as tested by Levene's test, we used log_{10} transformed data for analysis of POC quota, μ_c and Chl-a:POC ratios of *G. spinifera*, and for analysis of Chl-a:POC and ϵ_p of *S. trochoidea*.

Results

Elevated pCO$_2$ and light availability

In *G. spinifera*, μ_c did not change with CO_2 availability under LL, but increased under HL, which was mainly driven by increased POC quota in the highest CO_2 treatment (Fig 1A; linear regression; R^2 = 0.60; P = 0.003) (see also [17]). Moreover, μ_c was lower under LL (ANCOVA; P<0.001; 95% CI [-0.635; -1.026]), which was due to decreased POC quota in all CO_2 treatments, and due to lowered μ in all but the highest CO_2 treatment (Table 1). In *P. reticulatum*, μ_c was not affected by CO_2 under either LL or HL. Additionally, there was no interactive effect of CO_2 and light availability on μ_c. POC quota was unaffected by light in *P. reticulatum*, and significantly lower under LL in *G. spinifera* (ANCOVA; P<0.001; 95% CI [-1.024; 0.491]).

Ratios of Chl-a:POC increased with CO_2 in *P. reticulatum* under LL (Fig 1D; linear regression; R^2 = 0.45; P = 0.05), and were higher under LL for both *G. spinifera* and *P. reticulatum* (Fig 1C and 1D; ANCOVA; P<0.001; 95% CI [1.5; 1.1] and P<0.001; 95% CI [1.4; 1], respectively). Moreover, CO_2 and light availability showed interactive effects on the Chl-a:POC ratios (ANCOVA; $F_{1,20}$ = 9.453; P = 0.007 and $F_{1,19}$ = 9.149; P = 0.008, respectively). In other words, the effect of CO_2 depended on the light availability, with *P. reticulatum* showing a significant increase in Chl-a:POC ratios with CO_2 availability under LL only (linear regression; R^2 = 0.45; P = 0.05). Similarly, under LL Chl-a:POC ratios were significantly higher in the higher pCO$_2$ treatments of *G. spinifera* (ANOVA; P<0.05).

Under LL, ϵ_p increased with CO_2 in both *G. spinifera* and *P. reticulatum* (Fig 1E and 1F; linear regression; R^2 = 0.74; P = 0.003 and R^2 = 0.70; P = 0.005). Similar trends were observed under HL in *P. reticulatum* (linear regression; R^2 = 0.39; P = 0.04) and, for CO_2 levels between 180 and 800 µatm, also for *G. spinifera* (linear regression; R^2 = 0.79; P = 0.001; see also [16]). CO_2 and light showed interactive effects on ϵ_p in *G. spinifera* (ANCOVA; $F_{1,20}$ = 10.968; P = 0.004), and ϵ_p of cells grown under LL versus HL were only significantly different in the highest CO_2 treatment (>26; J-N; R^2 = 0.56; P = 0.02; Fig 1E). In *P. reticulatum*, low-light resulted in higher ϵ_p across the tested CO_2 concentrations (ANCOVA; P<0.001; 95% CI [1.7; 3.6]), with an average offset of 2.7‰.

Elevated pCO$_2$ and nitrogen-limitation

In *A. fundyense*, μ_c did not change with CO_2 when grown under either LN or HN. In *S. trochoidea*, μ_c was also independent of CO_2 under LN, while it decreased with CO_2 under HN (Fig 2B; linear regression; R^2 = 0.61; P = 0.003). In both *A. fundyense* and *S. trochoidea*, μ_c was lowered under LN, independent of the CO_2 concentration (Fig 2A and 2B; Table 2; ANCOVA; P<0.001; 95% CI [960; 1198] and P<0.001; 95% CI [-143; -321], respectively). LN did not affect POC quota in *A. fundyense*, but resulted in higher POC quota in *S. trochoidea* (ANCOVA; P<0.001; 95% CI [2591; 2261]).

Chl-a:POC ratios were interactively affected by CO_2 and nitrogen availability in *A. fundyense* (ANCOVA; $F_{1,17}$ = 13.393; P = 0.003), and cells grown under LN showed lower ratios at low CO_2 concentrations (i.e. <30 µmol L^{-1}; J-N; R^2 = 0.73; P<0.001). In *S. trochoidea*, Chl-a:

Fig 1. Combined effect of elevated pCO$_2$ and light-limitation. (A, B) POC production, (C, D) Chl-a:POC ratios and (E, F) ε_p versus CO$_2$ of *G. spinifera* (left) and *P. reticulatum* (right). Linear trend lines, R^2 and P-values represent statistically significant relationships. Symbols indicate means of technical replicates. Means ± SD for all treatments are provided in Table 1. Note that the trend line for *G. spinifera* under HL excludes the highest pCO$_2$ treatment (see also [16]). ε_p in the HL treatments have previously been published in Hoins et al. 2015.

doi:10.1371/journal.pone.0154370.g001

Table 1. Overview of the growth parameters in the HL and LL treatments. Growth rate (μ, d^{-1}), POC quota (pg C $cell^{-1}$), Chl-a content (pg $cell^{-1}$) and ^{13}C fractionation ε_p (‰) of *G. spinifera* and *P. reticulatum* grown under high-light and low-light conditions. Values represent the mean of triplicate incubations (n = 3 ±SD). Superscript letters indicate significant differences between pCO_2 treatments (P<0.05). Superscript symbols refer to earlier published data in Hoins et al. 2015 (*).

pCO_2 µatm	μ d^{-1}	POC quota pg C $cell^{-1}$	Chl a pg $cell^{-1}$	ε_p ‰
		G. spinifera <LL>		
380	0.19±0.03[a]	1743±271[a]	27.8±8.7[a]	7.8±0.1[a]
800	0.20±0.01[a]	2572±227[b]	66.2±3.3[b]	11.9±0.8[b]
1200	0.19±0.02[a]	2224±221[ab]	48.2±4.3[c]	13.7±1.5[b]
		G. spinifera <HL>		
180	0.22±0.02[a,*]	3708±366[a,*]	23.1±2.4[a]	7.8±1.0[a,*]
380	0.23±0.01[a,*]	2758±583[a,*]	19.1±1.7[a]	9.4±0.4[a,*]
800	0.23±0.04[a,*]	3521±263[a,*]	22.1±2.3[a]	11.7±0.7[b,*]
1200	0.15±0.01[b,*]	8842±1044[b,*]	32.6±6.0[b]	8.0±0.5[a,*]
		P. reticulatum <LL>		
380	0.25±0.01[a]	2843±233[a]	19.8±7.6[a]	10.9±0.5[a]
800	0.24±0.01[a]	2256±436[a]	26.6±3.9[b]	12.8±1.3[ab]
1200	0.27±0.01[a]	2552±204[a]	26.9±2.8[b]	13.7±0.6[b]
		P. reticulatum <HL>		
180	0.28±0.00[a,*]	3099±119[a,*]	9.7±0.3[a]	8.4±1.8[a,*]
380	0.28±0.01[a,*]	2494±356[ab,*]	5.7±0.9[a]	8.4±0.7[a,*]
800	0.29±0.02[a,*]	2351±694[b,*]	5.5±0.4[a]	8.6±2.3[a,*]
1200	0.29±0.03[a,*]	2600±316[ab,*]	6.2±0.7[a]	9.9±0.8[a,*]

doi:10.1371/journal.pone.0154370.t001

POC ratios were slightly lower under LN at all tested CO_2 concentrations (ANCOVA; P = 0.041; 95% CI [0.02; 0.6]). Under LN, POC:PON ratios were significantly higher in *S. trochoidea* in all tested pCO_2 treatments and in the lowest pCO_2 treatment of *A. fundyense* (ANOVA: P<0.05). POC:PON ratios were significantly lowered in the higher pCO_2 treatments of both species (ANOVA; P<0.05; Table 2) [19].

Under LN, ε_p was independent of CO_2 in both *A. fundyense* and *S. trochoidea* (Fig 2E and 2F), while there were positive correlations under HN (Fig 2E and 2F; linear regression; R^2 = 0.76; P<0.001 and R^2 = 0.77; P<0.001, respectively; see also [17]). In *A. fundyense*, CO_2 and nitrogen availability showed interactive effects on ε_p (ANCOVA; $F_{1,17}$ = 17.359; P = 0.001), with significantly higher ε_p values at lower CO_2 concentrations (i.e. <29 µmol L^{-1}; J-N; R^2 = 0.82, P<0.001). When grown under LN, both species show a relatively constant ε_p of around 13.0±0.6‰ in *A. fundyense* and 10.5±1.3‰ in *S. trochoidea*. These values are similarly high as the highest ε_p values obtained in the dilute batch cultures under HN (12.4±0.4 and 11.8±0.7‰, respectively).

Discussion

Production rates, quotas and stoichiometry

Our results show differential effects of elevated pCO_2 in combination with light availability on growth, POC quota, μ_c and Chl-a:POC ratios in *G. spinifera* and *P. reticulatum* (Fig 1; Table 1). In *G. spinifera*, μ_c increased with CO_2 under HL, but there was no sensitivity towards elevated pCO_2 under LL (Fig 1A). Low-light furthermore caused lowered POC quota and μ_c, while μ remained unaffected (Fig 1A and 1B; Table 1). At the same time, Chl-a contents and Chl-a: POC ratios increased under LL (Fig 1C and 1D; Table 1). Such higher ratios are needed to
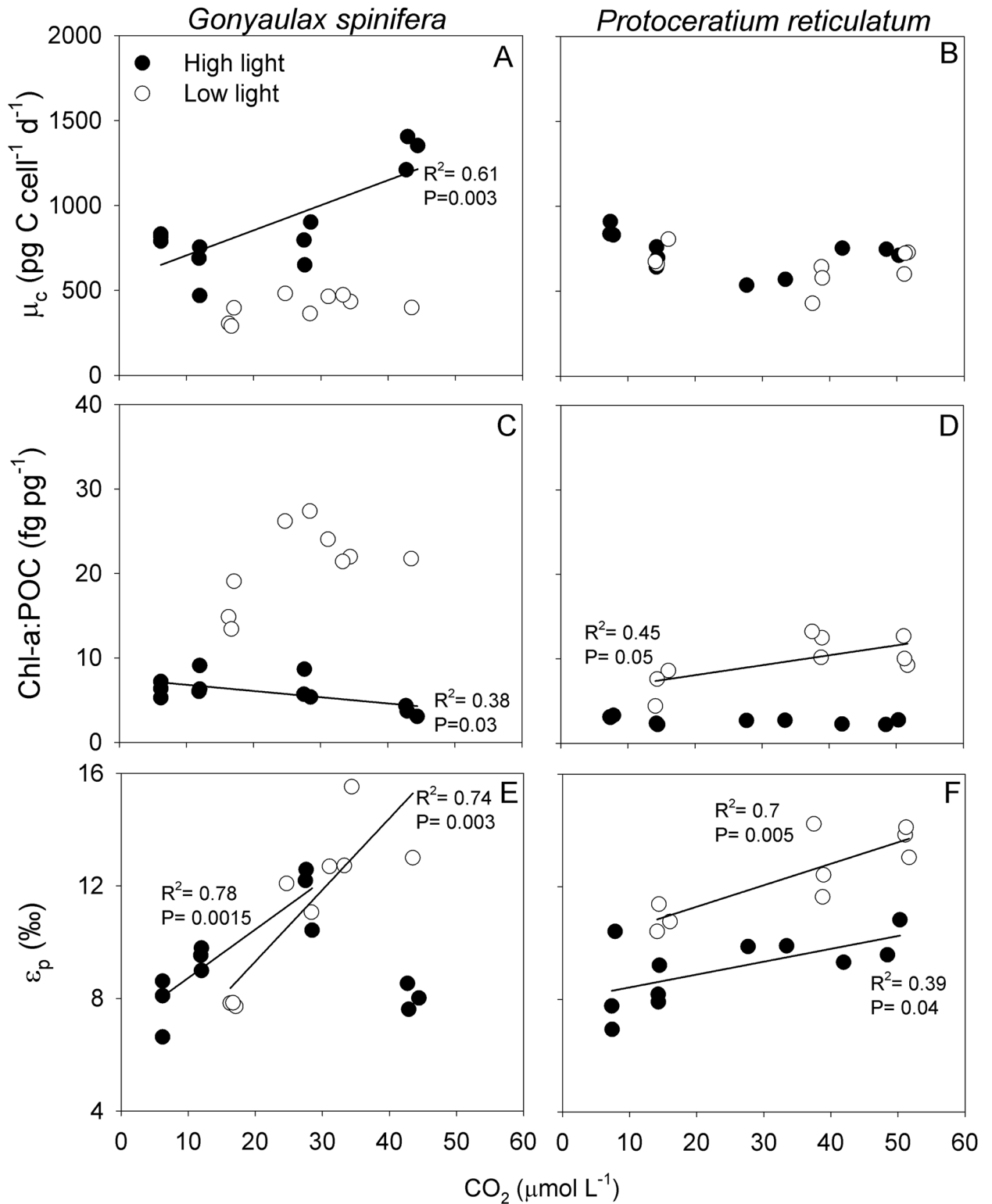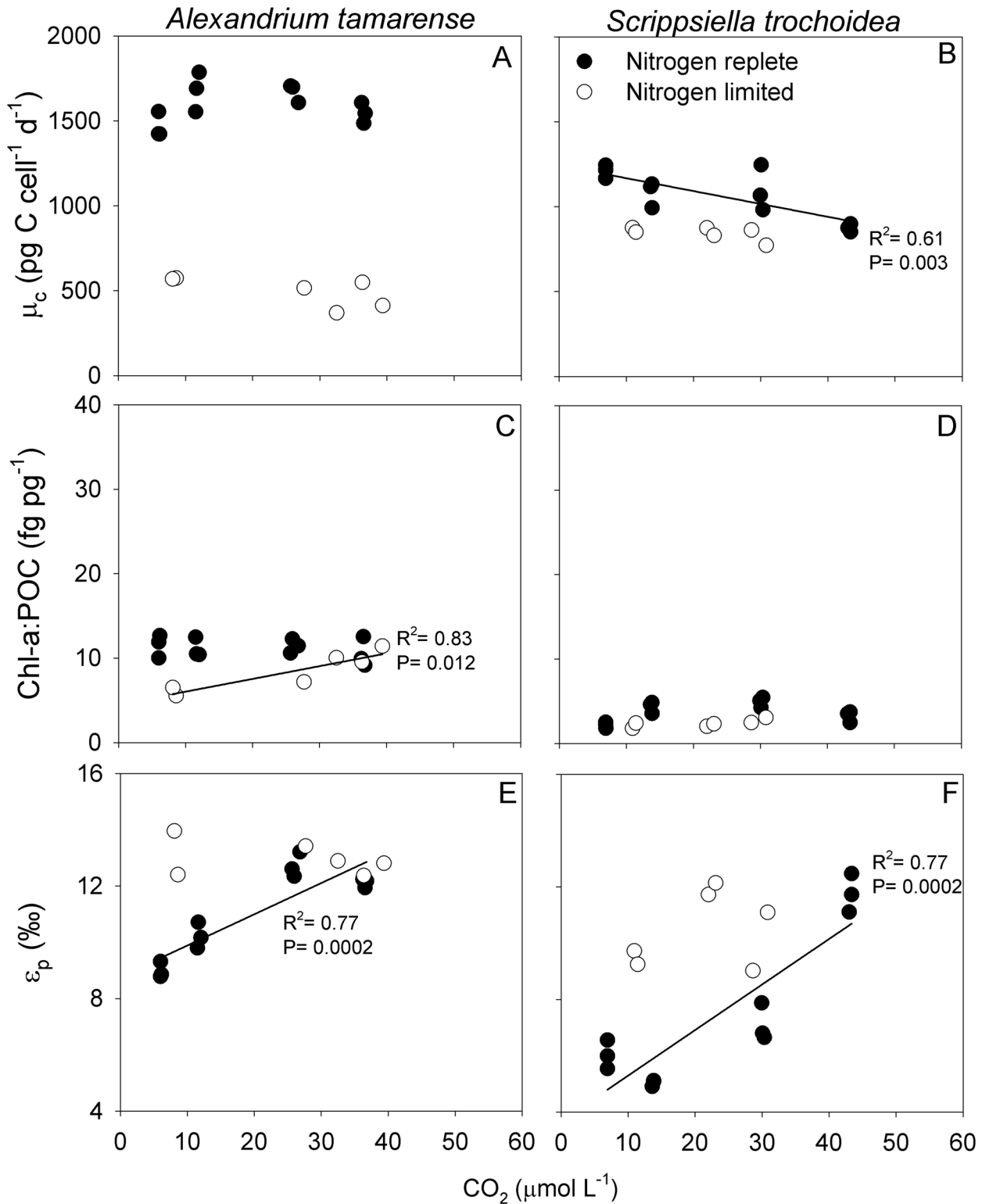
Fig 2. Combined effect of elevated pCO₂ and nitrogen-limitation. (A, B) POC production, (C, D) Chl-a:POC ratios and (E, F) ε_p versus CO_2 of A. fundyense (left) and S. trochoidea (right) cultured under nitrogen-replete conditions (HN; filled symbols) and nitrogen-limited conditions (LN; open symbols). Linear trend lines, R^2 and P-values represent statistically significant relationships. Symbols indicate means of technical replicates. Means ± SD for all treatments are provided in Table 2. POC production and Chl-a:POC ratios have previously been published in [15] and [18], and ε_p in the HN treatments in Hoins et al. 2015.

doi:10.1371/journal.pone.0154370.g002

Table 2. Overview of the growth parameters in the HN and LN treatments. Growth rate (μ, d^{-1}), POC quota (pg C $cell^{-1}$), Chl-a (pg $cell^{-1}$), POC:PON ratios (molar) and ε_p (‰) of *A. fundyense* and *S. trochoidea* grown under nitrogen-replete conditions and nitrogen-limitation. Values represent the mean of duplicate incubations (n = 2 ±SD). Superscript letters indicate significant differences between pCO$_2$ treatments (ANOVA; P<0.05; only applied when n>2). Superscript symbols refer to earlier published data in Hoins et al. 2015 (*), and Eberlein et al. 2014 (†) and 2016 (‡).

pCO$_2$ µatm	μ d^{-1}	POC quota pg C $cell^{-1}$	Chl-a pg $cell^{-1}$	POC:PON molar	ε_p ‰
		A. fundyense <LN>			
220	0.15±0.01[a,‡]	3930±212[a,‡]	22.9±2.0[a,‡]	9.52±0.46[a,‡]	13.18±1.1[a]
800	0.15±0.01[a,‡]	2709±253[b,‡]	24.7±0.6[a,‡]	6.75±0.16[b,‡]	13.15±0.4[a]
1000	0.15±0.01[a,‡]	3544±187[c,‡]	33.0±2.4[b,‡]	5.77±0.33[b,‡]	12.59±0.3[a]
		A. fundyense <HN>			
180	0.46±0.02[a,b,†]	3169±254[a,†]	36.3±1.5[a,†]	5.76±0.1[a,†]	9.0±0.3[a,*]
380	0.46±0.02[ab,†]	3620±308[a,†]	40.1±2.8[a,†]	5.77±0.3[a,†]	10.2±0.5[b,*]
800	0.48±0.01[a,†]	3455±153[a,†]	39.5±3.3[a,†]	5.73±0.1[a,†]	12.7±0.4[c,*]
1200	0.45±0.01[b,†]	3461±165[a,†]	36.4±5.8[a,†]	5.6±0.1[a,†]	12.1±0.2[c,*]
		S. trochoidea <LN>			
280	0.2±0.01[a‡]	4292±243[a,‡]	9.0±1.3[a,‡]	21.3±1.3[a,b,‡]	9.5±0.3[a]
590	0.2±0.01[a‡]	4239±220[a,‡]	9.2±0.6[a,‡]	24.7±1.6[b,‡]	11.9±0.3[a]
770	0.2±0.01[a‡]	4065±254[a,‡]	11.2±0.9[b,‡]	18.0±0.9[a,‡]	10.1±1.5[a]
		S. trochoidea <HN>			
180	0.61±0.03[a,†]	1990±36[a,†]	4.3±0.7[a,†]	7.6±0.2[ac,†]	6.0±0.5[ab,*]
380	0.61±0.05[a,†]	1762±15[ab,†]	7.6±1.2[ab,†]	8.1±0.3[ab,†]	5.0±0.1[a,*]
800	0.61±0.04[a,†]	1787±223[ab,†]	8.7±0.5[b,†]	8.4±0.3[b,†]	7.1±0.7[b,*]
1200	0.58±0.02[a,†]	1500±85[b,†]	4.9±1.3[a,†]	7.4±0.1[c,†]	11.8±0.7[c,*]

capture more light, which is a general response of phytoplankton to light-limitation. For *P. reticulatum*, the low light conditions did not yield changes in POC quota, μ and μ_c (Fig 1A and 1B; Table 1). This suggests a high flexibility of *P. reticulatum* to deal with low-light conditions. Cells did synthesize more Chl-a, thereby showing elevated Chl-a:POC ratios, which were apparently sufficient to compensate for the low-light conditions. Both species showed increasing Chl-a:POC ratios with increasing CO$_2$ availability when grown under low-light. This suggests that CO$_2$ influences the ability of cells to synthesize Chl-a, and therefore their ability to cope with low-light conditions.

We observed generally minor effects of elevated pCO$_2$ under LN, while nitrogen- limitation alone exerted a much stronger control (Fig 2, Table 2). Specifically, μ_c was lower in both *A. fundyense* and *S. trochoidea*, although POC quota in *S. trochoidea* grown under LN was significantly higher. Decreased μ_c was mainly a result of low μ, i.e. the imposed dilution rate which was set at about 33% of the μ of the respective species obtained from experiments under replete conditions. Nitrogen-limitation was confirmed by the higher POC:PON ratios in *S. trochoidea* in all tested pCO$_2$ treatments, while POC:PON ratios of *A. fundyense* grown under LN were only higher in the lowest pCO$_2$ treatment (Table 2) [19]. The Chl-a:POC ratios in LN were comparable to HN in *S. trochoidea*, while in *A. fundyense* these Chl-a:POC ratios showed a CO$_2$-dependent increase under LN, and only differed between HN and LN under low CO$_2$ concentrations. Thus, although nitrogen was limiting μ_c and caused an increase in POC:PON ratios, this did not strongly affect the Chl-a:POC ratios.

Irrespective of the light intensity or nitrogen concentration, CO$_2$ effects on growth rates, POC quotas and POC production in our study were either absent or relatively minor, suggesting the presence of effective carbon concentrating mechanisms (CCMs). Dinoflagellates possess RubisCO type II with lowest CO$_2$ affinities compared to all other eukaryotic algae [47; 48],

which make effective CCMs a prerequisite to maintain growth under low CO_2 concentrations. Indeed, earlier work has shown that *A. fundyense* and *S. trochoidea* are able to actively take up HCO_3^-, thus increasing their intracellular C_i pool [16]. Additionally, high extracellular activities of carbonic anhydrase, the enzyme accelerating the otherwise slow interconversion between CO_2 and HCO_3^-, have been found in *S. trochoidea* [16]. Consequently, at least the investigated dinoflagellate species do not seem to be CO_2-limited in any of tested CO_2 concentrations, irrespective of the light or nutrient supply, explaining why μ, POC quotas and μ_c did not respond to elevated CO_2 concentrations.

In the cyanobacterium *Trichodesmium* and the coccolithophore *Emiliania huxleyi*, limitation by light has been shown to cause enhanced sensitivity towards elevated pCO_2 [49; 50]. The CO_2-dependent stimulation of μ_c was most pronounced under light-limitation, which was explained by larger CO_2-dependent benefits due to the CCM down-regulation and thus energy reallocation under light-limitation. In the tested dinoflagellate species, however, μ_c remained largely unaltered over the applied CO_2 range (Figs 1A, 1B, 2A and 2B). Yet, we observed a CO_2-dependent increase in Chl-a:POC quota in *G. spinifera* and *P. reticulatum* grown under low-light. Thus, with elevated pCO_2 more energy is acquired via photosynthesis, while the same level of μ_c is maintained. It is further conceivable that their CCMs are down-regulated with elevated pCO_2, lowering the energetic costs for carbon acquisition. The likely higher availability of energy with elevated pCO_2 under low-light conditions, however, seems not to be allocated to μ_c (Figs 1C, 1D and 2C). This suggests either a lower overall efficiency to convert energy to biomass under these conditions, or a shunting of energy to alternative processes not accounted for in our study. Similarly to the Chl-a:POC ratios in *G. spinifera* and *P. reticulatum* under low-light conditions, Chl-a:POC ratios in *A. fundyense* grown under nitrogen-limitation also increased at elevated CO_2 concentrations. When grown under nitrogen-limitation, excess energy from a down-regulation of CCMs may be shunted to nitrogen acquisition. Indeed, POC:PON ratios decreased under elevated pCO_2 for both *A. fundyense* and *S. trochoidea* (Table 2) (see also [19]). Such lower POC:PON ratios (i.e. relatively more nitrogen) may favor synthesis of nitrogen-rich biomolecules such as Chl-a. Overall, elevated pCO_2 seems to have only minor effects on growth and μ_c in the tested dinoflagellates, and yet it apparently causes intracellular shifts in energy and resource allocation under light- or nitrogen-limited conditions.

^{13}C fractionation

The ^{13}C fractionation of phytoplankton is influenced by the interplay between 1) CO_2 supply, 2) inorganic carbon demand (i.e. μ_c), and 3) active uptake of CO_2 and HCO_3^- (i.e. CCMs). If CO_2 supply in the growth medium increases, ε_p increases because more of the ^{13}C-depleted CO_2 may be taken up in comparison to the ^{13}C-enriched HCO_3^-. In contrast, ε_p may decrease with increasing μ_c as CO_2 is fixed at a higher rate than total carbon is taken up, and the ability of RubisCO to express its full preference for $^{12}CO_2$ is reduced. CCMs can influence ε_p in various ways, e.g. as they determine the relative uptake of CO_2 and HCO_3^- as well as leakage (Fig 3). Under HL and HN conditions, ε_p shows a clear increase with increasing CO_2 concentrations in all four tested dinoflagellate species ([17]; Figs 1 and 2). Under LL, similar CO_2 dependencies were observed, although ε_p shifted to higher values in *P. reticulatum*. Under LN, ε_p was not CO_2 sensitive, and remained relatively high also at lower CO_2 concentrations for both *A. fundyense* and *S. trochoidea*.

Light- or nutrient-limitation cause changes in the availability of energy (ATP) and reductants (NADPH) that in turn may affect μ_c and CCM activity, eventually influencing ε_p (Fig 3). Under low-light conditions, for instance, less photons arrive at the photosystems, thereby

PROCESSES INFLUENCING ^{13}C FRACTIONATION

[1] *Leakage*: Refreshes the C_i pool, thereby increasing ^{13}C fractionation.

[2] *Diffusive CO_2 uptake*: Increases ^{13}C fractionation as CO_2 is ^{13}C-depleted.

[3] *POC production:* Increases the C_i fixation rate, thus lowering ^{13}C fractionation.

[4], [5] *Internal and external CA activity*: May affect ^{13}C fractionation in various ways as they accelerate the otherwise slow interconversion between CO_2 and HCO_3^-, thereby affecting leakage and relative CO_2 and HCO_3^- uptake.

[6] *Light:* May increase POC production, thereby potentially lowering ^{13}C fractionation. Light also fuels ATP production and thus CCM activity, thereby increasing or decreasing ^{13}C fractionation, depending on the C_i species that is actively taken up.

[7] *Nitrogen*: May increase POC production and linear electron flow (associated with HCO_3^- transport), thereby decreasing ^{13}C fractionation.

[8] *ATP:* Fuels CCMs, thereby potentially in- or decreasing ^{13}C fractionation.
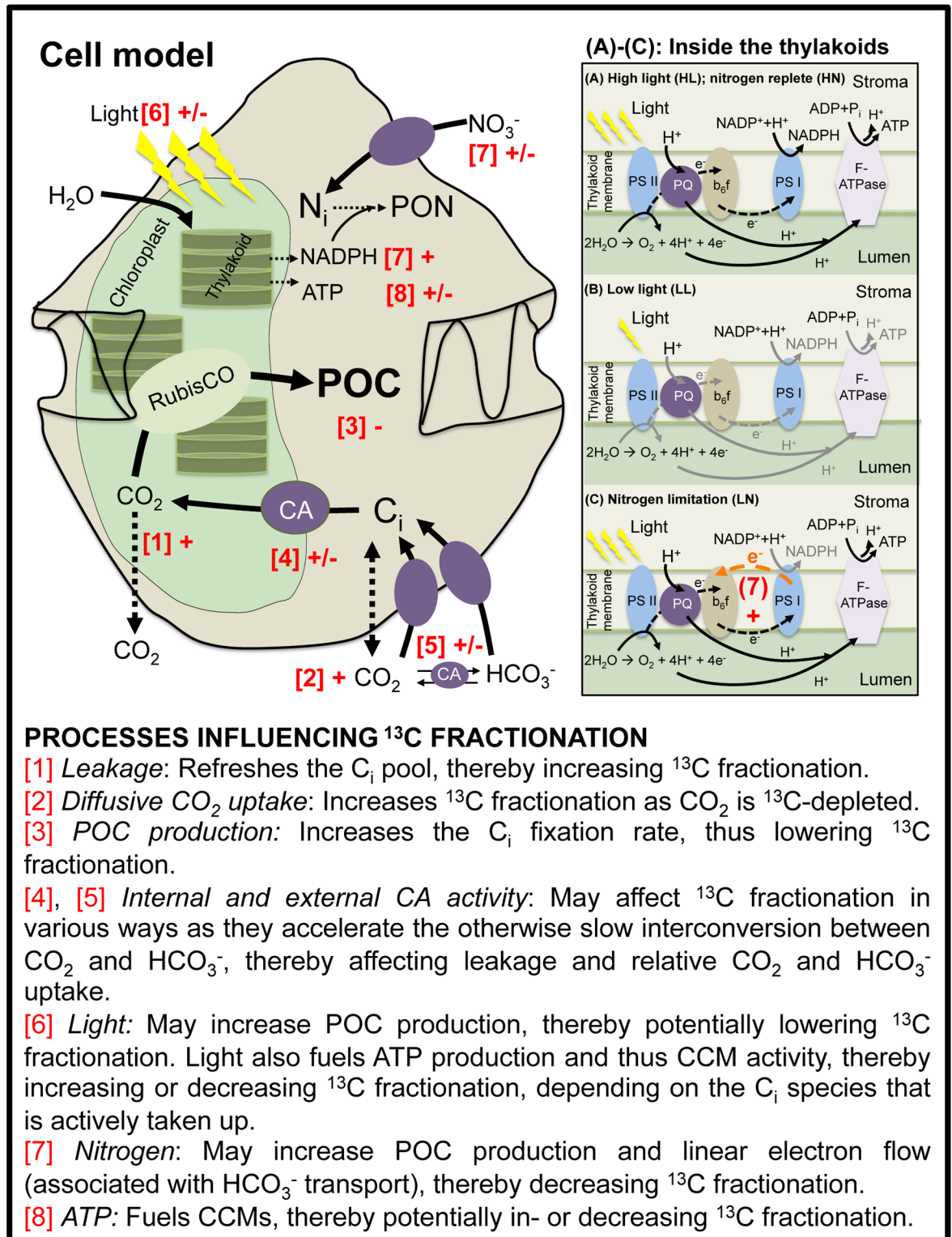
Fig 3. Conceptual model of a dinoflagellate cell and processes at the thylakoid membrane of the chloroplasts. (A) high-light (HL) and nitrogen-replete (HN) conditions, (B) low-light conditions (LL) and (C) nitrogen-limitation (LN). Processes potentially influencing ^{13}C fractionation ([1]–[8]) are highlighted in red, while + and – refer to an increase or decrease in ^{13}C fractionation, respectively. (A) Saturating light and nutrient-replete conditions: Light provides the energy (= photons) needed for Photosystem II (PSII; in thylakoid membrane) to oxidize water to O_2, thereby producing electrons (e^-) and protons (H^+).

Electrons are transported by plastohydroquinone (PQ), thereby pumping more protons into the lumen. The cytochrome b_6f complex oxidizes PQ molecules, thereby producing electrons, which are then transported to Photosystem I (PSI) where they reduce $NADP^+$ to NADPH. Protons are transported to F-ATPase to synthesize ATP. (B) Under light-limitation, the overall decreased amount of energy arriving at PSII causes a decrease in water oxidation, thereby producing less electrons and protons, and thus also less ATP and NADPH. (C) Under nitrogen-limitation, less NADPH is needed for NO_3^- reduction, thus the excess electrons are transported back to PSII by cyclic energy flow. Protons are still pumped by F-ATPase, thereby increasing the amount of ATP synthesized.

lowering the H_2O splitting and thus the production of electrons and protons (Fig 3B). The lowered electron and proton fluxes then result in lower amounts of ATP and NADPH. ATP is required to operate the energetically costly CCMs, while both ATP and NADPH are required for CO_2 reduction in the Calvin Cycle to produce biomass, and for reducing nitrate (NO_3^-) to ammonium (NH_4^+) to eventually produce particulate organic nitrogen (PON). Thus, differences in the availability of light but also nitrogen alter the availability of ATP and NADPH, which may be one reason for the differences in ε_p responses between types of incubations (e.g. [27; 51; 52; 30]).

High-light intensities may provide the cells with more energy than required for CO_2 fixation, which will enhance the active uptake of C_i that in turn serves as an energy sink for excess light [53]. Depending on how much C_i is taken up in relation to the amount of CO_2 that is fixed, a high C_i uptake may be accompanied by a high leakage [54]. A high C_i uptake by *G. spinifera* at both LL and HL, in concert with high leakage, would explain its relatively high ε_p. In contrast to our expectations, however, ε_p in *P. reticulatum* was substantially lower under HL conditions. In this species, an increasing contribution of energetically costly HCO_3^- uptake under HL may support the dissipation of excess energy, avoiding damage to photosystem II. If this active HCO_3^- uptake does not lead to higher leakage, it could in fact explain the lower ε_p under HL.

Comparable to light, also nitrogen availability may alter ε_p as it indirectly changes cellular energy budgets (Fig 3). As mentioned, NADPH is used to reduce CO_2 to organic carbon, and NO_3^- to NH_4^+. As a consequence, less NADPH is needed when μ_c is low and/or when NO_3^- is limiting. Under these conditions, cyclic electron flow "around" photosystem I may be up-regulated, thereby circumventing NADPH production while maintaining ATP generation (Fig 3C). Such a putative excess of ATP over NADPH, in turn, may be used for active inorganic carbon uptake. As ε_p in both *A. fundyense* and *S. trochoidea* was higher under nitrogen- limitation, CO_2 and not HCO_3^- may have been taken up actively. Alternatively, increasing overall C_i uptake despite low μ_c may have increased leakage and thus ε_p. Nonetheless, even the highest ε_p of ~14‰ in our study was low compared to earlier studies investigating the effect of nitrogen-limitation on ε_p in other algal species [27; 51; 28; 55]. This is in line with the generally high uptake of HCO_3^- observed in earlier studies on CCMs in dinoflagellates [14; 16]. Moreover, maximum ^{13}C fractionation of RubisCO in the tested dinoflagellate species may be lower than the typical 24–30‰, as was also found for a RubisCO isolated from *E. huxleyi* (i.e. 11‰; [56]).

Proxy development

The CO_2-dependency of ε_p in dinoflagellates can potentially serve in the development of a proxy for past pCO_2 in the atmosphere [17]. As indicated before, however, additional experiments focusing on environmental variables other than pCO_2, physiological underpinning of the recorded response, quantification of fractionation between dinoflagellate cells and cysts, as well as field calibration studies are required to establish a reliable proxy [17]. Here, we investigated the possible role of environmental variables other than pCO_2, including light and nitrogen availability.

The results show that under low-light conditions, the general response of ε_p towards elevated $p\text{CO}_2$ remains largely unaltered in *G. spinifera* and *P. reticulatum*, i.e. slopes remained largely similar. In contrast, ε_p becomes insensitive to changes in CO_2 under nitrogen-limitation in *A. fundyense* and *S. trochoidea*. Elevated $p\text{CO}_2$ in the past was presumable accompanied by water column stratification, thereby not only affecting the water depth at which dinoflagellates fixed carbon, but also the potential upwelling of nutrient-rich deeper water masses. Consequently, it is crucial to take into account the light conditions and nutrient concentrations during the dinoflagellate lifetime.

Application of an eventual proxy based on dinoflagellate ε_p would likely be most valuable at study sites where nitrate concentrations are non-limiting and stable through time. For such settings, the equilibrium between dissolved (recorded in dinoflagellates) and atmospheric (the proxy target) $p\text{CO}_2$ is typically sub-optimal. This results in an interesting paradox since study sites are required for which CO_2 is equilibrated between the ocean and atmosphere, and also bear sufficient nutrients to force a CO_2 response in ε_p. Moreover, intense blooms of dinoflagellates may deplete seawater not only in CO_2 [57; 58], but also in nutrients, leading to a potential bias in ε_p.

Thus, although ε_p shows largely consistent CO_2 dependencies across four tested dinoflagellate species under optimal growth conditions [16], other environmental factors, notably nitrogen limitation, complicate and possibly negate the suitability of dinoflagellate ε_p as a proxy for past $p\text{CO}_2$.

Supporting Information

S1 Appendix. Overview of the carbonate chemistry in all treatments. Average dissolved CO_2 concentrations (μmol L^{-1}), total alkalinity (TA: μmol L^{-1}), dissolved inorganic carbon (DIC; μmol L^{-1}) and pH (NBS scale). Values represent the mean ($\pm$SD) of triplicate incubations (n = 3), except for LN experiments which represent the mean of duplicate incubations (n = 2 $\pm$SD). Superscript letters indicate significant differences between $p\text{CO}_2$ treatments (ANOVA; $P<0.05$, only applied when n$>$2).
(DOCX)

Acknowledgments

Author Contributions

Conceived and designed the experiments: MH TE DBVDW BR AS GJR. Performed the experiments: MH TE DBVDW CHG KB. Analyzed the data: MH TE DBVDW. Contributed reagents/materials/analysis tools: MH TE DBVDW. Wrote the paper: MH DBVDW BR AS.

References

1. IPCC Fifth Assessment Report (AR5). Cambridge Univ. Press 2014

2. Wolf-Gladrow DA, Riebesell U, Burkhardt S, Bijma J. Direct effects of CO_2 concentration on growth and isotopic composition of marine plankton. Tellus B Chem Phys Meterol. 1999; 51(2): 461–476.

3. Boyd PW, Doney SC. Modelling regional responses by marine pelagic ecosystems to global climate change. Geophys Res Lett. 2002; 29(16): 53–1.

4. Behrenfeld MJ, O'Malley RT, Siegel DA, McClain CR, Sarmiento JL, Boss ES et al. Climate-driven trends in contemporary ocean productivity. Nature 2006; 444(7120): 752–755. PMID: 17151666

5. Polovina JJ, Mitchum GT, Evans GT. Decadal and basin-scale variation in mixed layer depth and the impact on biological production in the Central and North Pacific, 1960–88. Deep Sea Res Part I: Oceanogr Res Pap. 1995; 42(10): 1701–1716.

6. Doney SC. Oceanography: Plankton in a warmer world. Nature 2006; 444(7120): 695–696. PMID: 17151650

7. Cembella AD. Occurrence of okadaic acid, a major diarrhetic shellfish toxin, in natural populations of *Dinophysis spp*. from the eastern coast of North America. J Appl Phycol. 1989; 1(4): 307–310.

8. Anderson DM, Glibert PM, Burkholder JM. Harmful algal blooms and eutrophication: nutrient sources, composition, and consequences. Estuaries 2002; 25(4): 704–726.

9. Steidinger KA, Landsberg JH, Flewelling LJ, Kirkpatrick BA. Toxic dinoflagellates. Oceans and Human Health; Risks and Remedies From the Seas 2008: 239–56.

10. Jeong HJ, Du Yoo Y, Kim JS, Seong KA, Kang NS, Kim TH. Growth, feeding and ecological roles of the mixotrophic and heterotrophic dinoflagellates in marine planktonic food webs. Ocean Sci. 2010; 45(2): 65–91.

11. John U, Tillmann U, Hülskötter J, Alpermann TJ, Wohlrab S, Van de Waal DB. Intraspecific facilitation by allelochemical mediated grazing protection within a toxigenic dinoflagellate population. P Roy Soc Lond B Bio. 2015; 282 (1798), [20141268]

12. Wall D, Dale B. Modern dinoflagellate cysts and evolution of the Peridiniales. Micropaleontology 1968: 265–304.

13. Brading P, Warner ME, Davey P, Smith DJ, Achterberg EP, Suggett DJ. Differential effects of ocean acidification on growth and photosynthesis among phylotypes of Symbiodinium (Dinophyceae). Limnol Oceanogr. 2011; 56(3), 927–938.

14. Rost B, Richter KU, Riebesell U, Hansen PJ. Inorganic carbon acquisition in red tide dinoflagellates. Plant Cell Environ. 2006; 29: 810–822. PMID: 17087465

15. Hansen PJ, Lundholm N, Rost B. Growth limitation in marine red-tide dinoflagellates: effects of pH versus inorganic carbon availability. Mar Ecol-Prog Ser. 2007; 334: 63–71.

16. Eberlein T, Van de Waal DB, Rost B. Differential effects of ocean acidification on carbon acquisition in two bloom-forming dinoflagellate species. Physiol Plantarum 2014: doi: 10.1111/ppl.12137

17. Hoins M, Van de Waal DB, Eberlein T, Reichart GJ, Rost B, Sluijs A. Stable carbon isotope fractionation of organic cyst-forming dinoflagellates: evaluating the potential for a pCO_2 proxy. Geochim Cosmochim Ac 2015; 160: 267–276.

18. Burkhardt S, Riebesell U, Zondervan I. Stable carbon isotope fractionation by marine phytoplankton in response to daylength, growth rate, and CO_2 availability. Marine Ecol- Prog Ser. 1999a; 184: 31–41.

19. Eberlein T, Van de Waal DB, Brandenburg KM, John U, Voss M, Achterberg EP, Rost B. Interactive effects of ocean acidification and nitrogen-limitation on two bloom-forming dinoflagellate species. Conditionally accepted at Mar Ecol-Prog Ser. 2015.

20. Roeske CA, O'Leary MH. Carbon isotope effects on enzyme-catalyzed carboxylation of ribulose bisphosphate. Biochemistry 1984; 23(25): 6275–6284.

21. Raven JA, Johnston AM. Mechanisms of inorganic-carbon acquisition in marine phytoplankton and their implications for the use of other resources. Limnol Oceanogr. 1991; 36: 1701–1714.

22. Guy RD, Fogel ML, Berry JA. Photosynthetic fractionation of the stable isotopes of oxygen and carbon. Plant Physiol. 1993; 101(1): 37–47. PMID: 12231663

23. Sharkey TD, Berry JA. Carbon isotope fractionation of algae as influenced by an inducible CO_2 concentrating mechanism. In Lucas WJ and Berry JA [eds.], Inorganic carbon uptake by aquatic photosynthetic organisms. Plant Physiol. 1985: 389–401.

24. Burkhardt S, Riebesell U, Zondervan I. Effects of growth rate, CO_2 concentration, and cell size on the stable carbon isotope fractionation in marine phytoplankton. Geochim Cosmochim Ac. 1999b; 63: 3729–3741.

25. Van de Waal DB, John U, Ziveri P, Reichart GJ, Hoins M, Rost B et al. Ocean acidification reduces growth and calcification in a marine dinoflagellate. PLoS ONE 8 2013: e65987. doi: 10.1371/journal. pone.0065987 PMID: 23776586

26. Fensome RA, Taylor FJR, Norris G, Sarjeant WAS, Wharton DI, Williams GL. A Classification of Modern and Fossil Dinoflagellates. Micropaleontology 1993; Special Publication 7: Sheridan Press, Hanover, 351.

27. Laws EA, Bidigare RR, Popp BN. Effect of growth and CO_2 concentration on carbon isotope fractionation by the marine diatom *Phaedactylum tricornutum*. Limnol Oceanogr. 1997; 42: 1552–1560.

28. Bidigare RR, Fluegge A, Freeman KH, Hanson KL, Hayes JM, Wakeham SG et al. Consistent fractionation of ^{13}C in nature and in the laboratory: Growth-rate effects in some haptophyte algae. Global Biogeochem Cy. 1997; 11: 279–292.

29. Riebesell U, Burkhardt S, Dauelsberg A, Kroon B. Carbon isotope fractionation by a marine diatom: dependence on the growth-rate-limiting resource. Marine Ecol-Prog Ser. 2000; 193: 295–303.

30. Rost B, Zondervan I, Riebesell U. Light dependent carbon isotope fractionation in the coccolithophorid *Emiliania huxleyi*. Limnol Oceanogr. 2002; 47: 120–128.

31. Tillmann U, Alpermann TL, da Purificação RC, Krock B, Cembella A. Intra-population clonal variability in allelochemical potency of the toxigenic dinoflagellate Alexandrium fundyense. Harmful Algae 2009; 8: 759–769.

32. John U, Litaker RW, Montresor M, Murray S, Brosnahan ML, Anderson DM. Formal revision of the *Alexandrium tamarense* species complex (Dinophyceae) taxonomy: the introduction of five species with emphasis on molecular-based (rDNA) classification. Protist 2014; 165(6), 779–804. doi: 10.1016/j. protis.2014.10.001 PMID: 25460230

33. Keller MD, Selvin RC, Claus W, Guillard RRL. Media for the culture of oceanic ultraplankton. J Phycol. 1987; 23: 633–638.

34. Guillard RRL, Ryther JH. Studies of marine planktonic diatoms. *I. Cyclotella* nana Hustedt and *Detonula confervacea* (Cleve) Gran. Can J of Microbiol. 1962; 8: 229–239.

35. Van de Waal DB, Eberlein T, Bublitz Y, John U, Rost B. Shake it easy: a gently mixed continuous culture system for dinoflagellates. J Plankton Res. 2014; 36(3): 889–894.

36. Pierrot DE, Lewis E, Wallace DWR. Program Developed for CO_2 System Calculations. Carbon Dioxide Information Analysis Center, Oak Ridge National Laboratory 2006; Available at: http://cdiac.ornl.gov/oceans/co2rprt.html

37. Hoppe CJM, Langer G, Rokitta SD, Wolf-Gladrow DA, Rost B. Implications of observed inconsistencies in carbonate chemistry measurements for ocean acidification studies. Biogeosciences 2012; 9: 2401–2405.

38. Mehrbach C, Culberson CH, Hawley JE, Pytkowicz RM. Measurement of the apparent dissociation constants of carbonic acid in seawater at atmospheric pressure. Limnol Oceanogr. 1973; 18: 897–907.

39. Dickson AG, Millero FJ. A comparison of the equilibrium constants for the dissociation of carbonic acid in seawater media. Deep Sea Res Part I: Oceanogr Res Pap. 1987; 34: 1733–1743.

40. Dickson AG. Standard potential of the reaction: AgCl(s) + 1/2H_2(g) = Ag(s) + HCl(aq), and the standard acidity constant of the ion HSO4- in synthetic seawater from 273.15 to 318.15 K.J. Chem Thermodyn. 1990; 22: 113–127.

41. Knap AH, Michaels A, Close AR, Ducklow H, Dickson AG. Protocols for the joint global ocean flux study (JGOFS) core measurements. JGOFS 1996; Reprint of the IOC Manuals and Guides No. 29, UNESCO 1994, 19.

42. Freeman KH, Hayes JM. Fractionation of carbon isotopes by phytoplankton and estimates of ancient CO_2 levels. Glob Biogeochem Cy. 1992; 6: 185–198.

43. Zeebe RE, Wolf-Gladrow DA. CO_2 in Seawater: Equilibrium, Kinetics, Isotopes 2001; Amsterdam, The Netherlands: Elsevier Science.

44. Mook WG, Bommerson JC, Staverman WH. Carbon isotope fractionation between dissolved bicarbonate and gaseous carbon dioxide. Earth Planet Sci Lett. 1974; 22: 169–176.

45. Zhang J, Quay PD, Wilbur DO. Carbon isotope fractionation during gas-water exchange and dissolution of CO_2. Geochim Cosmochim Ac. 1995; 59: 107–114.

46. Johnson PO, Neyman J. (1936) Tests of certain linear hypotheses and their application to some educational problems. Statistical research memoirs. 1936.

47. Badger MR, Andrews TJ, Whitney SM, Ludwig M, Yellowlees DC, Price GD et al. The diversity and coevolution of Rubisco, plastids, pyrenoids, and chloroplast-based CO_2-concentrating mechanisms in algae. Can J of Bot. 1998; 76(6): 1052–1071.

48. Whitney SM, Andrews TJ. The CO_2/O_2 specificity of single subunit ribulose bisphosphate carboxylase from the dinoflagellate *Amphidinium carterae*. Aust J of Plant Physiol. 1998; 25: 131–138.

49. Kranz SA, Levitan O, Richter KU, Prášil O, Berman-Frank I, Rost B. Combined effects of CO_2 and light on the N_2-fixing cyanobacterium *Trichodesmium* IMS101: Physiological responses. Plant Physiol. 2010; 154: 334–345. doi: 10.1104/pp.110.159145 PMID: 20625004

50. Rokitta SD, Rost B. Effects of CO_2 and their modulation by light in the life-cycle of the coccolithophore *Emiliania huxleyii*. Limnol Oceanogr. 2012; 5(2): 607–618.

51. Laws EA, Popp BN, Bidigare RR, Kennicut MC, Macko SA. Dependence of phytoplankton carbon isotopic composition on growth rate and $[CO_2]_{aq}$: Theoretical considerations and experimental results. Geochim Cosmochim Ac. 1995; 59: 1131–1138.

52. Rau GH, Riebesell U, Wolf-Gladrow DA. A model of photosynthetic ^{13}C fractionation by marine phytoplankton based on diffusive molecular CO_2 uptake. Mar Ecol-Prog Ser. 1996; 133: 275–285.

53. Tchernov D, Hassidim M, Luz B, Sukenik A, Reinhold L, Kaplan A. Sustained net CO_2 evolution during photosynthesis by marine microorganism. Curr Biol. 1997; 7(10): 723–728. PMID: 9368754

54. Tchernov D, Silverman J, Luz B, Reinhold L, Kaplan A. Massive light-dependent cycling of inorganic carbon between oxygen photosynthetic microorganisms and their surroundings. Photosynth Res. 2003; 77: 95–103. PMID: 16228368

55. Popp BN, Laws EA, Bidigare RR, Dore JE, Hanson KL, Wakeham SG. Effect of phytoplankton cell geometry on carbon isotopic fractionation. Geochim Cosmochim Ac. 1998; 62: 69–77.

56. Boller AJ, Thomas PJ, Cavanaugh CM, Scott KM. Low stable carbon isotope fractionation by coccolithophore RubisCO. Geochim Cosmochim Ac. 2011; 75(22); 7200–7207.

57. Hansen PJ. Effect of high pH on the growth and survival of marine phytoplankton: implications for species succession. Aquat microb ecol. 2002; 28(3): 279–288.

58. Hinga KR. Effects of pH on coastal marine phytoplankton. Mar Ecol-Prog Ser. 2002; 238: 281–300.